PHYSICAL REVIEW B **68**, 220504(R) (2003)

Superconductivity near the vibrational-mode instability in $MgCNi_3$

A. Yu. Ignatov, S. Y. Savrasov, and T. A. Tyson
Department of Physics, New Jersey Institute of Technology, Newark, New Jersey 07102, USA
(Received 13 October 2003; published 23 December 2003)

To understand the role of electron-phonon interaction in superconducting $MgCNi_3$ we have performed density-functional based linear response calculations of its lattice dynamical properties. A large coupling constant $\lambda = 1.51$ is predicted and contributing phonons are identified as displacements of Ni atoms towards octahedral interstitials of the perovskite lattice. Instabilities found for some vibrational modes emphasize the role of anharmonic effects in resolving experimental controversies.

DOI: 10.1103/PhysRevB.68.220504 PACS number(s): 74.25.Jb, 61.50.Ks, 74.70.Ad

The discovery of superconductivity in $MgCNi_3$[1] has generated a new puzzle in the recent series of found superconductors.[2] Despite its relatively low T_c (8 K), the presence of Ni signals the possible importance of correlation effects which makes the physics of the pairing mechanism relevant to the famous high-T_c cuprates and brings the discussion of unconventional non-electron-phonon mechanism. The experimental information characterizes $MgCNi_3$ as moderate[1,3] or strong-coupling[4] conventional superconductor through the analysis of specific-heat data, supports the *s*-wave pairing by nuclear magnetic resonance experiments,[5] and at the same time shows a zero-bias anomaly in tunneling data.[4] A clear need for detailed information about the phonon spectra emerges from these controversial data in order to clarify the role of electron-phonon interaction (EPI) and understand the mechanism of superconductivity.

In this work, we perform theoretical studies of the strength of the electron-phonon coupling in $MgCNi_3$ by using fully self-consistent density-functional based linear response calculations[6] of the lattice dynamical properties as a function of phonon wave vector **q**. This method was proven to provide reliable estimates for the phonon spectra and electron-phonon interactions in a large variety of systems.[6,7]

The basic element of the perovskite $MgCNi_3$ structure is given by a carbon atom placed at the center of the cube and octahedrally coordinated by six Ni atoms. Our electronic structure calculation using full potential linear muffin-tin orbital (LMTO) method[8] reveals Ni-*d* C-*p* hybridized valence bands $\epsilon_{\mathbf{k}j}$ in accord with the previous studies.[9–11] The Fermi-surface consists of several sheets such as rounded cube sections centered at Γ, thin jungle gym area spanning from $R\ [\frac{1}{2}\frac{1}{2}\frac{1}{2}]2\pi/a$ to $M\ [\frac{1}{2}\frac{1}{2}0]2\pi/a$ points, dimpled square shaped hole pockets centered around X point $[\frac{1}{2}00]2\pi/a$, as well as little ovoids along $\Gamma - R$. The tight-binding picture discussed before[9] consists of carbon $p_x\ p_y\ p_z$ orbitals hybridized with *d* states of three Ni atoms numerated accordingly as Ni_x Ni_y and Ni_z. For example (see Fig. 1), carbon p_z state hybridizes with $Ni_z\ d_{z^2-1}$ and also with $Ni_x\ d_{xz}$ $Ni_y\ d_{yz}$. Similar picture holds for carbon p_x, p_y orbitals which are not shown. As it has been noted,[9] this in particular results in two antibonding states crossing the Fermi level, which in the nearest-neighbor approximation have no dispersion along some directions in the Brillouin zone (BZ).

The appearance of nearly flat areas of $\epsilon_{\mathbf{k}j}$ gives rise to two-dimensional (2D) van Hove singularity (vHS) placed 40 meV below the Fermi energy ϵ_F, which is responsible for a strong narrow peak near ϵ_F. This has generated speculation about closeness of $MgCNi_3$ to ferromagnetic instability upon doping.[9–12] The narrowness of the vHS band is controlled by the second-nearest-neighbor hopping integrals, which for the states shown in Fig. 1 correspond to the overlap between Ni_x and Ni_y d_{xy} orbitals. As we discuss in this work, nearly unstable phonon modes exists when each of the two Ni atoms moves toward octahedral interstitial sites. (This is shown in Fig. 1 by arrows for a phonon wave vector $\mathbf{q} = [\frac{1}{2}\frac{1}{2}0]2\pi/a$.) We shall see that these distortions wipe out the narrow vHS peak and give rise to a large electron-phonon coupling.

To calculate lattice dynamics of $MgCNi_3$ as a function of wave vector **q** we utilize the linear response method,[6,8] We use 2κ LMTO basis set, generalized gradient approximation for exchange correlation,[13] experimental lattice constant $a = 7.206$ a.u., as well as effective (40,40,40) grid in **k** space (total 1771 irreducible **k** points) to generate the phonon dispersions $\omega_{\mathbf{q}\nu}$ and electron-phonon matrix elements $g_{\mathbf{k}+\mathbf{q}j'\mathbf{k}j}$

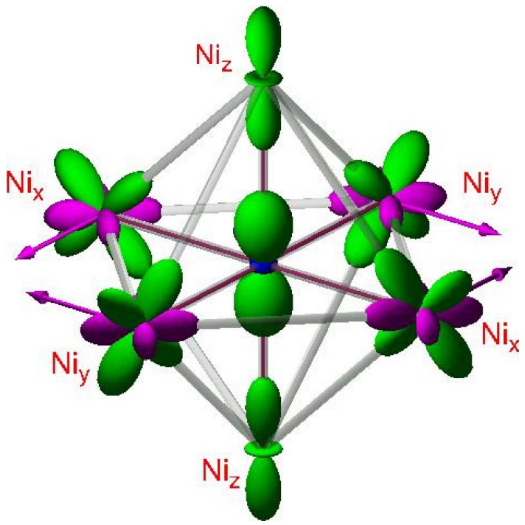

FIG. 1. Basic element of the structure and set of tight-binding orbitals relevant to low-energy physics $MgCNi_3$. Arrows show displacements of Ni atoms corresponding to wavevector $\mathbf{q} = [\frac{1}{2}\frac{1}{2}0]2\pi/a$.

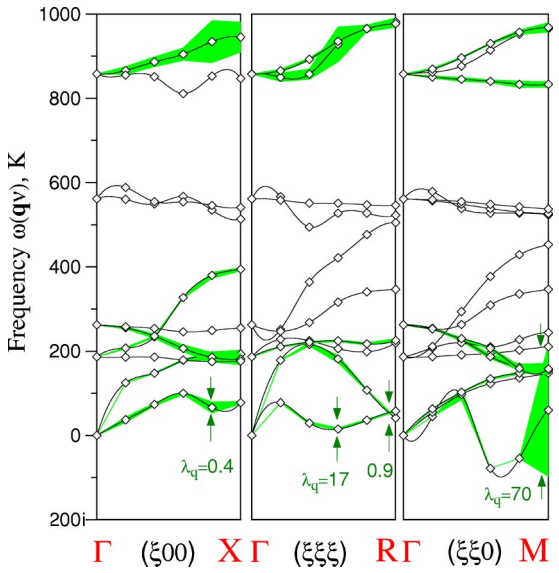

FIG. 2. Calculated phonon spectrum of $MgCNi_3$ using density-functional linear response method. Some curves are widened proportionally to the phonon linewidths.

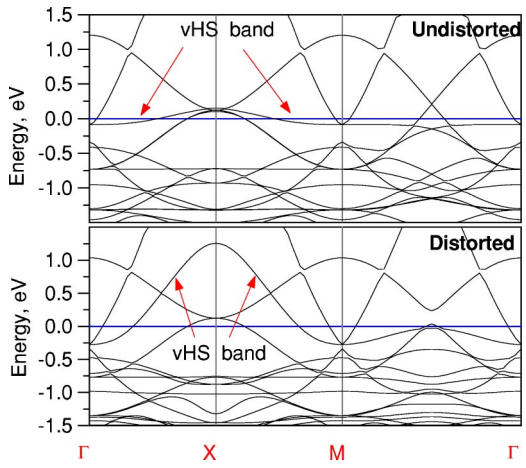

FIG. 3. Calculated one-electron structure corresponding to the Ni based frozen phonon with $\mathbf{q}=[\frac{1}{2}\frac{1}{2}0]2\pi/a$. Top panel—undistorted bands, bottom panel—distorted bands corresponding to the Ni displacements by 0.2 Å.

on a (10,10,10) grid of the **q** vectors (total 56 irreducible **q** points).

Our calculated phonon spectrum along major high symmetry lines of the cubic Brillouin zone is given on Fig. 2. The frequencies are seen to be span up to 900 K, with some of the modes showing significant dispersion. In general, we distinguish three panels where the top three branches around 900 K are carbon based, the middle three branches around 600 K are Mg based and nine lower branches are all Ni based. For the Γ point *z*-polarized modes, in particular, consist of (i) Ni_z-C against Mg-Ni_x-Ni_y vibrations (186 K), (ii) pure Ni_x-Ni_y vibrations (262 K), (iii) Mg against Ni_x-Ni_y (561 K), (iv) C against Ni_z vibrations (857 K).

A striking feature of this phonon spectrum is the presence of a low-frequency acoustic mode which is very soft and is even seen to be unstable along $(\xi\xi 0)$ direction in the BZ. This mode is essentially Ni based and corresponds to perpendicular movements of two Ni atoms towards octahedral interstitials of the perovskite structure. The latter is made of each of the four Ni atoms and two Mg atoms. For example, considering the *xy* plane (see Fig. 1) for the **q** point *M* such movements can be seen as a 2D breathing around this vacant interstitial. We find a similar situation for other wave vectors and in other directions of the BZ, where each pair of Ni atoms prefers such in-phase displacements perpendicular to each other. The softness and instability here can be understood as the octahedral interstitials are only places to escape for each Ni atom stressed between two surrounding carbons.

The discussed displacements affect the overlap integrals between nearest Ni t_{2g} orbitals which control the width of the vHS band. For the *xy* plane these are the hoppings between d_{xy} orbitals (see Fig. 1). It is therefore clear that these modes should have large EPI.

To illustrate the crucial change in the electronic structure due to such distortions, Fig. 3 shows two one-electron spectra in the vicinity of the Fermi level corresponding to the *M* point frozen phonon involving Ni_x displacement along the *y* axis in phase with the Ni_y displacement along the *x* axis as illustrated on Fig. 1. The top panel of Fig. 3 corresponds to the undistorted energy bands drawn in the original cubic BZ for easier comparison with the published data.[9–11] As the point $[\frac{1}{2}\frac{1}{2}0]2\pi/a$ is now a reciprocal vector of the new doubled lattice, the bands are seen to be simply folded, and the narrow vHS band is readily recognized. When we introduce a distortion by 0.2 Å, the only essential difference is the width of the vHS band which now disperses as much as 1.5 eV. The smallness of the assumed displacement emphasizes the large electron-phonon coupling. Its appearance cannot be understood from a simple geometric overlap between the two t_{2g} orbitals (d_{xy} states between Ni_x and Ni_y shown in Fig. 1). We therefore look for an electronic enhancement due to nestinglike features of the Fermi surface. Indeed, such nesting can be found for the two dimpled square shaped hole pockets centered at *X* separated exactly by the wave vector $[\frac{1}{2}\frac{1}{2}0]2\pi/a$. We have confirmed that feature by corresponding calculation of the integral $\Sigma_{\mathbf{k}jj'}\delta(\epsilon_{\mathbf{k}j}-\epsilon_F)\delta(\epsilon_{\mathbf{k}+\mathbf{q}j}-\epsilon_F)$ which provides the total phase space available for the electrons to scatter at given wave vector **q** with no energy change.

We now turn our discussion to the detailed dependence of the electron-phonon coupling across the entire BZ. This at least can be done for all stable phonons. Figure 2 shows the calculated phonon linewidths $\gamma_{\mathbf{q}\nu}$ by widening some representative dispersion curves $\omega_{\mathbf{q}\nu}$ proportionally to $\gamma_{\mathbf{q}\nu}$. Each phonon linewidth is proportional to[14] $\Sigma_{\mathbf{k}jj'}|g^{\mathbf{q}\nu}_{\mathbf{k}+\mathbf{q}j'\mathbf{k}j}|^2\delta(\epsilon_{\mathbf{k}j}-\epsilon_F)\delta(\epsilon_{\mathbf{k}+\mathbf{q}j}-\epsilon_F)$, where the electron-phonon matrix element is found self-consistently from the linear response theory.[6] In particular, we see that some phonons have rather large linewidths. This, for example, holds for all carbon based higher-lying vibrational modes. The strength of the coupling $\lambda_{\mathbf{q}\nu}$ for each mode can be obtained by dividing $\gamma_{\mathbf{q}\nu}$ by $\pi N(\epsilon_F)\omega^2_{\mathbf{q}\nu}$, where $N(\epsilon_F)$ is the density of states at the Fermi level equal to 5.3 st./[eV*cell] in our calculation.

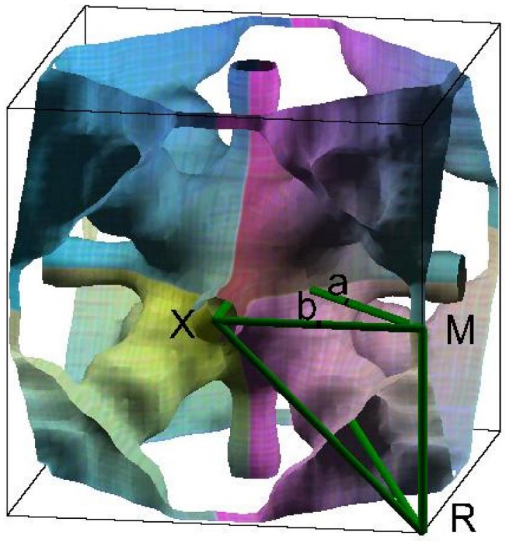

FIG. 4. Surface in the Brillouin zone which separates stable and instable areas for the Ni based acoustic mode.

Due to large $\omega^2_{\mathbf{q}\nu}$, this unfortunately results in strongly suppressed coupling for all carbon modes which would favor high critical temperatures. The coupling, however, is relatively strong for the Ni based modes. For example, we can find λ's of the order of 1–3 for the Ni based optical phonons around 250 K. Again, the analysis of the polarization vectors shows that these vibrations involve Ni movements towards octahedral interstitials. For example (see Fig. 1), the movement of Ni_x and Ni_y atoms along the z direction either in-phase or out-of-phase result in larger overlap between Ni_z Ni_y d_{yz} orbitals and between Ni_z Ni_x d_{xz} orbitals. Similar to what we find for the M point using the frozen-phonon method (Fig. 3), this again enlarges the vHS bandwidth resulting in large EPI. An extremely large coupling ($\lambda \sim 70$) occurs for the soft acoustic mode involving the interstitial breathing (M point). Here we point out a triple effect: (i) breathing of four Ni_x Ni_y atoms into the interstitial, which results in larger d_{xy} overlap, (ii) nesting enhancement which helps wiping out the vHS peak, and (iii) the smallness of $\omega^2_{\mathbf{q}\nu}$. As the linewidth of this particular phonon is so large, the concept of phonon itself has to be questioned, but due to a smallness of the phase space associated with this vibration, this has a little effect on integral characteristics such as λ.

Unfortunately, finding the integral value of λ is another challenging problem due to the appearance of the imaginary frequencies. Neglecting the unstable mode completely results in the average coupling constant equal to 0.95 mainly due to the discussed Ni vibrations around 250 K (see Fig. 2). It is however clear that the low-frequency mode has a large contribution to λ and cannot be omitted. For which wave vectors $\mathbf{q}$ this mode is unstable? Since we know its dispersion across the entire BZ, we can determine a surface in $\mathbf{q}$ space which separates the real and imaginary frequencies. Figure 4 shows the result of such an analysis. We see the area around the Γ point which continues along the lines towards the R,M, and X points. Here we find the stability of the mode. The area around the M point, where we find enormously large EPI, is seen to be very small . This is also clear from the dispersion relations shown in Fig. 2 for the $(\xi\xi 0)$ direction, where the frequency becomes real just near the M point itself.

This instability carefully avoids symmetry points which can be understood by keeping in mind the symmetry of the discussed distortions. Namely, anharmonicity is expected to be large for all in-plane movements involving two, three, or four Ni atoms towards octahedral interstitials. This is forbidden near the Γ point and for all wave vectors $(\xi 00)$ along ΓX as well as for $(\xi\xi\xi)$ along ΓR directions if, for example, xy plane is considered. It is however allowed for $(\xi\xi 0)$ along ΓM and for $(\frac{1}{2}\xi 0)$ along XM. Moreover, for the wave vectors with $q_z \neq 0$, the displacements away from xy plane are allowed and the instability is quickly suppressed. This, e.g., is the case of $(\frac{1}{2}\frac{1}{2}\xi)$ along MR.

The persistence of the instability which does not occur for any of the high-symmetry point needs a nontrivial frozen-phonon analysis. As our polarization vectors promt that the largest anharmonicity is expected for the ΓXM plane with $q_z = 0$, we have performed three such calculations for the points $a=(\frac{1}{4}\frac{1}{4}0)2\pi/a$, $b=(\frac{1}{2}\frac{1}{4}0)2\pi/a$, and M shown in Fig. 4. This corresponds to the discussed displacements of two (point a), three (point b), or four (point M) Ni atoms within xy plane. The results of these calculations reveal essentially anharmonic interatomic Ni potentials. A shallow double well with a depth of the order of 10–40 K and the curvature at the equilibrium of the order of 40–50i K exists for the a and b points which becomes vanishing at the M point. We have found such a behavior by both total energy and force calculations for the supercells of 20 atoms (a and b points) and 10 atoms (M point). Clearly, such a small depth on the temperature scale indicates that the distortions are dynamical and zero point motions would prevent the appearance of the static long-range order. This picture is confirmed by our recent extended x-ray absorbtion fine spectroscopy experiments (EXAFS), which reveal dynamical distortions[15] not seen in the conventional diffraction experiments. Remarkably that the parameters of the double well (depth 10 K and the equilibrium curvature 50i K) extracted from EXAFS are in accord with our frozen-phonon data.

It is now clear that our instable mode is not related to a statically distorted structure of $MgCNi_3$ but should be resolved using an anharmonic theory of the EPI. Using a combination of our frozen-phonon and linear response data we are able to map the behavior of the instable mode inside the entire Brillouin zone using a (4,4,4) grid of $\mathbf{q}$ vectors. This gives us a possibility to determine a contribution to the Eliashberg spectral function using a generalized formula[16,17]

$$\alpha^2 F(\omega) = \frac{1}{N(\epsilon_F)} \sum_{\mathbf{q}} \sum_{\mathbf{k}j\mathbf{k}'j'} \sum_{n} \delta[\omega - \omega_n(\mathbf{q})] \times \frac{[f_{\mathbf{k}j} - f_{\mathbf{k}'j'}]\delta[\epsilon_{\mathbf{k}j} - \epsilon_{\mathbf{k}'j} + \omega_n(\mathbf{q})]|G^{(n)}_{\mathbf{k}'j'\mathbf{k}j}(\mathbf{q})|^2}{[\omega_n(\mathbf{q})]^2}, \tag{1}$$

where the summation over the eigenstates n of the anharmonic oscillator appears here with $\omega_n(\mathbf{q}) = \epsilon_n(\mathbf{q}) - \epsilon_0(\mathbf{q})$ be-

ing the excitation frequencies around the ground-state level for the anharmonic well at a given wave vector **q**. The generalized electron-phonon matrix element $G^{(n)}_{\mathbf{k}'j'\mathbf{k}j}(\mathbf{q})$ involves transitions from the ground to nth excited state and also includes changes in the effective one-electron potential to all orders with respect to the displacements. The most important is the effect of the frequency renormalization which appears in denominator of Eq. (1). As we find, our anharmonic mode has the first excitation frequency which, depending on the **q** point, varies from 120 to 150 K. We also find that the summation over n is fastly convergent in accord with the previous work:[16] the oscillator strength for $n=2$ is always less than 2% of that for $n=1$. The linear electron-phonon scattering matrix elements are known to us from the linear response calculations, and numerically small corrections due to second-order couplings have been extracted from our frozen-phonon data using the band splittings technique.[17]

Our resulting value of λ for this anharmonic mode appears to be 0.56. Adding the result for $\lambda=0.95$ from all other modes our total λ is now 1.51. This is consistent with the values of λ extracted from specific-heat measurements[1,3,18] and would cause $MgCNi_3$ to be a strongly coupled electron-phonon superconductor.

To estimate T_c, we solve the Eliashberg equation with our total (harmonic+anharmonic) $\alpha^2F(\omega)$. The cutoff frequency ω_{cut} is taken to be ten times the maximum phonon frequency. The Coulomb pseudopotential $\mu^*(\omega_{cut})$ is varied and T_c within the range 7–20 K is obtained. Making connection to the μ^* that is usually used in Allen-Dynes modified McMillan T_c formula[19] the rescaling expression $[\mu^*]^{-1}=[\mu^*(\omega_{cut})]^{-1}+\ln(\omega_{cut}/\omega_{\max})$ is utilized.[20] We found that both the experimental T_c and the superconducting energy gap $\Delta(0)$ can be reproduced with the value of $\mu^*=0.33$. While the effect of spin fluctuations on superconductivity and mass enhancement is better to discuss in terms of its own coupling constant λ_{spin}, at the absence of detailed calculation of the latter, we can only conclude that our enhanced μ^* can, in principle, appear due to localized nature of Ni d orbitals. In fact, at the absence of spin fluctuations, μ^* is usually 0.1–0.15 and T_c in $MgCNi_3$ could be larger. We conclude that spin fluctuations partially suppress superconductivity, the result expected from the conventional theory. Note that the same conclusion has been reached based on the recent analysis of the specific-heat data.[18] We finally calculated the phonon contribution to the specific heat and fitted it to the form $C(T)=\beta T^3$ at low temperatures. Our value of $\beta=0.35$ mJ/[mol*K^4] is close to the values 0.40–0.42 mJ/[mol*K^4] determined experimentally.[3,4,18]

In conclusion, by performing linear response calculations of the electron-phonon interaction in $MgCNi_3$ we reported the value of $\lambda=1.51$ consistent with the strong-coupling limit of electron-phonon mechanism of superconductivity. An unusually large anharmonic correction to λ for the lattice near instability is emphasized.

We thank O. V. Dolgov, I. I. Mazin, and W. Pickett for useful comments, and S. Shulga for availability of his programs to solve Eliashberg's equations. The work was supported by the grants NSF DMR Nos. 9733862, 0209243, 0238188, 0342290, U.S. Department of energy No. DE-FG02-99ER45761, NJSGC No. 02-42.

[1] T. He, Q. Huang, A.P. Ramirez, Y. Wang, K.A. Regan, N. Rogado, M.A. Hayward, M.K. Haas, J.S. Slusky, K. Inumara, H.W. Zandbergen, N.P. Ong, and R.J. Cava, Nature (London) **411**, 54 (2001).

[2] J. Nagamatsu, N. Nakagawa, T. Muranaka, Y. Zenitani, and J. Akimitsu, Nature (London) **410**, 63 (2001); S.S. Saxena and P.B. Littlewood, *ibid.* **412**, 290 (2001); R. Matzdorf, Z. Fang, Ismail, J. Zhang, T. Kimura, Y. Tokura, K. Terakura, and E.W. Plummer, Science **289**, 746 (2000).

[3] J.-Y. Lin, P.L. Ho, H.L. Huang, P.H. Lin, Y.-L. Zhang, R.-C. Yu, C.-Q. Jin, and H.D. Yang, Phys. Rev. B **67**, 052501 (2003).

[4] Z. Mao, M.M. Rosario, K. Nelson, K. Wu, I.G. Deac, P. Schiffer, Y. Liu, T. He, K.A. Regan, and R.J. Cava, Phys. Rev. B **67**, 094502 (2003).

[5] P.M. Singer, T. Imai, T. He, M.A. Hayward, and R.J. Cava, Phys. Rev. Lett. **87**, 257601 (2001).

[6] S.Y. Savrasov, Phys. Rev. Lett. **69**, 2819 (1992); S.Y. Savrasov, D.Y. Savrasov, and O.K. Andersen, *ibid.* **72**, 372 (1994).

[7] S.Y. Savrasov and O.K. Andersen, Phys. Rev. Lett. **77**, 4430 (1996); S.Y. Savrasov and G. Kotliar *ibid.* **90**, 056401 (2003).

[8] S.Y. Savrasov, Phys. Rev. B **54**, 16 470 (1996).

[9] D.J. Singh and I.I. Mazin, Phys. Rev. B **64**, 140507(R) (2001).

[10] S.B. Dugdale and T. Jarlborg, Phys. Rev. B **64**, 100508(R) (2001).

[11] J.H. Shim, S.K. Kwon, and B.I. Min, Phys. Rev. B **64**, 180510(R) (2001).

[12] H. Rosner, R. Weht, M.D. Johannes, W.E. Pickett, and E. Tosatti, Phys. Rev. Lett. **88**, 027001 (2002).

[13] J.P. Perdew, K. Burke, and M. Ernzerhof, Phys. Rev. Lett. **77**, 3865 (1996).

[14] P.B. Allen, Phys. Rev. B **6**, 2577 (1972).

[15] A.Yu. Ignatov, L.M. Dieng, T.A. Tyson, T. He, and R.J. Cava, Phys. Rev. B **67**, 064509 (2003).

[16] J.C.K. Hui, and P.B. Allen, J. Phys. F: Met. Phys. **4**, L42 (1974).

[17] V. Meregalli and S.Y. Savrasov, Phys. Rev. B **57**, 14 453 (1998).

[18] A. Waelte, H. Rosner, M.D. Johannes, G. Fuchs, K.-H. Mueller, A. Handstein, K. Nenkov, V.N. Narozhnyi, S.-L. Drechsler, S. Shulga, and L. Schultz, cond-mat/0208364 (unpublished).

[19] P.B. Allen and R.C. Dynes, Phys. Rev. B **12**, 905 (1975).

[20] J.P. Carbotte, Rev. Mod. Phys. **62**, 1027 (1990).